

SELF-ATTENTION NETWORKS FOR CONNECTIONIST TEMPORAL CLASSIFICATION IN SPEECH RECOGNITION

Julian Salazar*

Katrin Kirchhoff*†

Zhiheng Huang*

*Amazon AI

†University of Washington

{julsal, katrinki, zhiheng}@amazon.com

ABSTRACT

Self-attention has demonstrated great success in sequence-to-sequence tasks in natural language processing, with preliminary work applying it to end-to-end encoder-decoder approaches in speech recognition. Separately, connectionist temporal classification (CTC) has matured as an alignment-free strategy for monotonic sequence transduction, either by itself or in various multitask and decoding frameworks. We propose SAN-CTC, a deep, fully self-attentional network for CTC, and show it is tractable and competitive for speech recognition. On the Wall Street Journal and LibriSpeech datasets, SAN-CTC trains quickly and outperforms existing CTC models and most encoder-decoder models, attaining 4.7% CER in 1 day and 2.8% CER in 1 week respectively, using the same architecture and one GPU. We motivate the architecture for speech, evaluate position and downsampling approaches, and explore how the label alphabet affects attention head and performance outcomes.

Index Terms— speech recognition, connectionist temporal classification, self-attention, multi-head attention, end-to-end

1. INTRODUCTION

Connectionist temporal classification (CTC) [1] has matured as a scalable, alignment-free approach for *monotonic* sequence transduction tasks such as handwriting recognition [2], action labeling [3], and automatic speech recognition (ASR) [1, 4–11]. In ASR, CTC sidesteps the label alignment procedure required by previous hidden Markov model / neural network (HMM-NN) approaches [12]. The most successful end-to-end approach to *general* sequence transduction, however, is the encoder-decoder framework [13] with attention [14]. While initially employed in machine translation, its generality has made it amenable to ASR as well [15–20]. However, its lack of enforced monotonicity makes encoder-decoder ASR models difficult to train, often leveraging many thousands of hours of data [18], careful learning rate schedules [19], pretraining [20], and/or auxiliary CTC losses [17, 20, 21] for state-of-the-art results.

Both frameworks have conventionally used recurrent layers to model temporal dependencies. As this hinders parallel processing, further works proposed partially- or purely-convolutional CTC models [8–11] and convolution-heavy encoder-decoder models [16] for ASR. However, convolutional models must be significantly deeper to retrieve the same temporal receptive field [22]. Recently, the mechanism of *self-attention* [23, 24] was proposed, which views the whole sequence at once and models interactions between features that are arbitrarily distant in time. Using it in both encoder-decoder and feed-forward contexts has led to faster training and state-of-the-art results in translation (in particular, the Transformer [24]), sentiment analysis [25], and other tasks. These successes have motivated preliminary work in self-attention for ASR. Time-restricted self-attention

was used as a drop-in replacement for individual layers in the state-of-the-art lattice-free MMI model [26], an HMM-NN system. The effectiveness of hybrid self-attention/LSTM encoders was studied in the context of listen-attend-spell (LAS) [27], an encoder-decoder system. Finally, direct adaptations of the Transformer to speech have been demonstrated in [19, 28, 29].

Our work is the first to propose and evaluate self-attention in the CTC framework (SAN-CTC). Beyond continuing this body of work in end-to-end ASR, we are motivated by practical considerations: SAN-CTC can be used as a drop-in architectural replacement to improve CTC-based systems; unlike the Transformer, SAN-CTC also predicts tokens in parallel during inference; an analysis of SAN-CTC will be useful for future state-of-the-art ASR systems, which might equip self-attentive encoders with auxiliary CTC losses [17, 20]. Unlike other works, we do not require convolutional frontends [19] or interleave with recurrences [27]. In Section 2, we motivate the model and the relevant design choices (position, downsampling) for ASR. In Section 3, we validate SAN-CTC on the Wall Street Journal and LibriSpeech datasets by outperforming existing CTC models and most encoder-decoder models in character error rate (CERs), with fewer parameters or less training time. Finally, we evaluate our model with respect to different label alphabets (character, phoneme, subword), we use WFST decoding to give word error rates (WERs) as needed, and we examine the learned attention heads for insights.

2. MODEL ARCHITECTURES FOR CTC AND ASR

Consider an input sequence of T feature vectors, viewed as a matrix $\mathbf{X} \in \mathbb{R}^{T \times d_{\text{fr}}}$. Let \mathbb{L} denote the (finite) label alphabet, and denote the output sequence as $\mathbf{y} = (y_1, \dots, y_U) \in \mathbb{L}^U$. In ASR, \mathbf{X} is the sequence of acoustic frames, \mathbb{L} is the set of graphemes/phonemes/wordpieces, and \mathbf{y} is the corresponding ground-truth transcription over \mathbb{L} .

For CTC, one assumes $U \leq T$ and defines an intermediate alphabet $\mathbb{L}' = \mathbb{L} \cup \{-\}$, where ‘-’ is called the *blank symbol*. A *path* is a T -length sequence of intermediate labels $\boldsymbol{\pi} = (\pi_1, \dots, \pi_T) \in \mathbb{L}'^T$. Paths are related to output sequences by a many-to-one mapping that collapses repeated labels then removes blank symbols:

$$\mathcal{B} : \mathbb{L}'^T \rightarrow \mathbb{L}^{\leq T}, \text{ e.g., } (a, b, -, -, b, b, -, a) \mapsto (a, b, b, a). \quad (1)$$

Hence, paths are analogous to framewise alignments in the HMM-NN framework. In this way, CTC can model the distribution of sequences by marginalizing over all paths corresponding to an output:

$$P(\mathbf{y} \mid \mathbf{X}) = \sum_{\boldsymbol{\pi} \in \mathcal{B}^{-1}(\mathbf{y})} P(\boldsymbol{\pi} \mid \mathbf{X}). \quad (2)$$

Here, CTC models $P(\boldsymbol{\pi} \mid \mathbf{X})$ as a sequence of conditionally-independent outputs:

$$P(\boldsymbol{\pi} \mid \mathbf{X}) = \prod_{t=1}^T P(\pi_t, t \mid \mathbf{X}). \quad (3)$$

This model assumption, along with the monotonicity implied by \mathcal{B} , allows $\mathcal{L}_{\text{CTC}}(\mathbf{X}, \mathbf{y}) = -\log P(\mathbf{y} \mid \mathbf{X})$ to be computed efficiently with dynamic programming [1, 4] for maximum likelihood estimation (MLE) based training via gradient descent.

2.1. Recurrent and convolutional models

In practice, one uses a neural network to model $P(\pi, t \mid \mathbf{X})$. As inspired by HMMs, the model simplification of conditional independence can be tempered by multiple layers of (recurrent) bidirectional long short-term memory units (BLSTMs) [1–4]. However, these are computationally expensive (Table 1), leading to simplifications such as gated recurrent units (GRUs) [8, 30]; furthermore, the success of the $\text{ReLU}(x) = \max(0, x)$ nonlinearity in preventing vanishing gradients enabled the use of vanilla bidirectional recurrent deep neural networks (BRDNNs) [5, 6, 31] to reduce operations per layer.

Convolutions over time and frequency were first used as initial layers to recurrent neural models, beginning with HMM-NNs [32] and later with CTC, where they are viewed as promoting invariance to temporal and spectral translation in ASR [8], or image translation in handwriting recognition [33]; they also serve as a form of dimensionality reduction (Section 2.3). However, these networks were still bottlenecked by the sequentiality of operations at the recurrent layers, leading [8] to propose row convolutions for unidirectional RNNs, which had finite lookaheads to enable online processing while preserving some future context.

Ultimately, this led to purely-convolutional CTC architectures for capturing long-range temporal dependencies [9–11] with no sequentiality per layer. However, these models have to be very deep (e.g., 17–19 convolutional layers on LibriSpeech [22]) to cover the same context (Table 1). While in theory, a relatively local context suffices for ASR, this is complicated by alphabets \mathbb{L} which heavily violate the conditional independence assumption of CTC (e.g., English characters [34]). Wide contexts also enable the incorporation of noise and speaker characteristics; [27] saw attention heads with broad ranges emerge naturally in the first layer of their self-attentional LAS models.

2.2. Self-attention

We now consider replacing recurrent and convolutional layers in the CTC architecture with self-attention [23]. The building block of our proposed network (SAN-CTC) is the *self-attention layer* (Figure 1), as defined in the encoder of the Transformer [24] and used in previous explorations of self-attention in speech [19, 27]. It is composed of two *sublayers* with residual connections and layer normalizations (LN) in between (Figure 1).

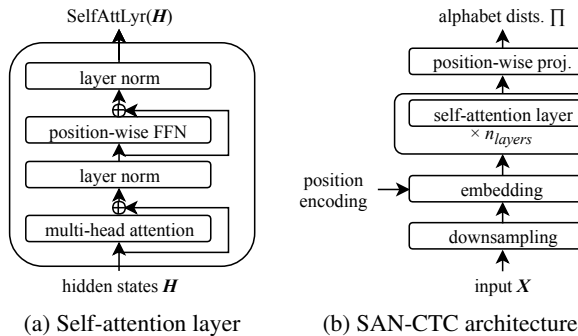


Fig. 1: Self-attention in the CTC framework

Let $\mathbf{H} \in \mathbb{R}^{T \times d_h}$ denote a sublayer's input. The first sublayer performs *multi-head, scaled dot-product self-attention* [24]. For each head $1 \leq i \leq n_{\text{hds}}$ (a number which divides into d_h), we learn linear projections $\mathbf{W}_Q^{(i)}, \mathbf{W}_K^{(i)} \in \mathbb{R}^{d_h \times d_k}, \mathbf{W}_V^{(i)} \in \mathbb{R}^{d_h \times d_h/n_{\text{hds}}}$. Left multiplication by \mathbf{H} give the *queries* $\mathbf{Q}^{(i)}$, *keys* $\mathbf{K}^{(i)}$, and *values* $\mathbf{V}^{(i)}$ of the i -th head, respectively. Each head computes

$$\mathbf{HdAtt}^{(i)} = \sigma \left(\mathbf{Q}^{(i)} \mathbf{K}^{(i)\top} / \sqrt{d_h} \right) \mathbf{V}^{(i)}, \quad (4)$$

where σ is row-wise softmax. Heads are concatenated along the d_h/n_{hds} axis to give $\mathbf{MltHdAtt} = [\mathbf{HdAtt}^{(1)}, \dots, \mathbf{HdAtt}^{(n_{\text{hds}})}]$. The second sublayer is a *position-wise, feed-forward network* [24] $\mathbf{FFN}(\mathbf{H}) = \text{ReLU}(\mathbf{H}\mathbf{W}_1 + \mathbf{b}_1)\mathbf{W}_2 + \mathbf{b}_2$ where parameters $\mathbf{W}_1 \in \mathbb{R}^{d_h \times d_{\text{ff}}}, \mathbf{b}_1 \in \mathbb{R}^{d_{\text{ff}}}, \mathbf{W}_2 \in \mathbb{R}^{d_{\text{ff}} \times d_h}, \mathbf{b}_2 \in \mathbb{R}^{d_h}$ are learned, with the biases $\mathbf{b}_1, \mathbf{b}_2$ broadcasted over all T positions. This sublayer aggregates the multiple heads at time t into the attention layer's final output at t . All together, the layer is given by:

$$\mathbf{MidLyr}(\mathbf{H}) = \text{LN}(\mathbf{MltHdAtt}(\mathbf{H}) + \mathbf{H}), \quad (5)$$

$$\mathbf{SelfAttLyr}(\mathbf{H}) = \text{LN}(\mathbf{FFN}(\mathbf{MidLyr}(\mathbf{H})) + \mathbf{MidLyr}(\mathbf{H})). \quad (6)$$

Note that the query $\mathbf{Q}_{t,:}$ uses its dot product with each key in \mathbf{K} to produce a weighted sum over values \mathbf{V} . One analogy this suggests is that attention heads are akin to large, content-parameterized, convolutional filters. Since the ‘filter weights’ are not fixed, fewer heads suffice. Furthermore, the flexibility of these heads helps make them ‘interpretable’; for example, [27] observes their LAS self-attention heads to be acting as phoneme detectors. Finally, this view of a head as a generalized convolution suggests that a stack of self-attention layers could, in principle, automatically learn the gradual increase of receptive field that convolutional CTC models are hardcoded with. Further design biases like filter widths and causality could then be incorporated through *time-restricted self-attention* [26] and *directed self-attention* [25], respectively.

Model	Operations per layer	Sequential operations	Maximum path length
Recurrent	$O(Td^2)$	$O(T)$	$O(T)$
Convolutional	$O(kTd^2)$	$O(1)$	$O(T/k)$
Convolutional (strided/dilated/pooled)	$O(kTd^2)$	$O(1)$	$O(\log_k(T))$
Self-attention	$O(T^2d)$	$O(1)$	$O(T)$
Self-attention (restricted)	$O(kTd)$	$O(1)$	$O(T/k)$

Table 1: Operation complexity of each layer type, based on [24]. T is input length, d is no. of hidden units, and k is filter/context width.

These layers are integrated into SAN-CTC along with related stages (Figure 1): *downsampling*, which reduces the size of T via one of the methods of Section 2.3; *embedding*, which learns an embedding into d_h that incorporates position via one of the encodings in Section 2.4; and *projection*, whereby the final d_h is projected by a dense layer into framewise logits over the intermediate alphabet \mathbb{L}' .

2.3. Downsampling

In speech, the input length T of frames can be many times larger than the output length U , in contrast to the original use case of the Transformer (machine translation). This is especially prohibitive for self-attention in terms of memory: recall that an attention matrix of dimension $\mathbf{Q}^{(i)} \mathbf{K}^{(i)\top} \in \mathbb{R}^{T \times T}$ is created, giving the T^2

factor in Table 1. A convolutional frontend is a typical downsampling strategy [8, 19]; however, we leave combining SAN-CTC with other layer types as future work. Instead, we consider three fixed approaches, from least to most preserving of the input data: *subsampling*, which only takes every k -th frame; *pooling*, which aggregates every k consecutive frames via a statistic (average, maximum); *reshaping*, where one concatenates k consecutive frames into one [27]. Note that CTC will still require $U \leq T/k$, however.

2.4. Position

Self-attention is inherently content-based [24], and so one often encodes position into the post-embedding vectors. We use standard trigonometric embeddings, where for $0 \leq i \leq d_{\text{emb}}/2$, we define

$$\text{PE}(t, 2i) = \sin \frac{p}{10000^{2i/d_{\text{emb}}}}, \quad \text{PE}(t, 2i + 1) = \cos \frac{p}{10000^{2i/d_{\text{emb}}}}.$$

We will consider three approaches: *content-only* [21], which forgoes position encodings; *additive* [19], which takes $d_{\text{emb}} = d_h$ and adds the encoding to the embedding; and *concatenative*, where one takes $d_{\text{emb}} = 40$ and concatenates it to the embedding. The latter was found necessary for self-attentional LAS [27], as additive encodings failed to converge. However, the monotonicity of CTC is itself a significant positional prior, which should enable even content-only training to be successful.

3. EXPERIMENTS

We take $(n_{\text{layers}}, d_h, n_{\text{heads}}, d_{\text{ff}}) = (10, 512, 8, 2048)$, giving $\sim 30\text{M}$ parameters. This is on par with models on WSJ (10-30M) [4, 5, 9] and an order of magnitude below models on LibriSpeech (100-250M) [8, 22]. We use MXNet [35] for modeling and Kaldi/EESEN [7, 36] for data preparation and decoding. Our self-attention code is based on the GluonNLP toolkit implementation. At train time, utterances are sorted by length: we exclude those longer than 1800 frames ($\ll 1\%$ of each training set). We take a window size of 25ms, a hop size of 10ms, and concatenate features with their temporal first- and second-order differences. We downsample by a factor of $k = 3$ (this also gives an ideal $T/k \approx d_h$ for our data; see Table 1).

We perform Nesterov-accelerated gradient descent on batches of 20 utterances. As self-attention architectures can be unstable in early training, we clip gradients by a global norm of 1 and use the standard linear warmup period before inverse square decay associated with these architectures [19, 24]. Let n denote the global step number of the batch (across epochs); the learning rate is then given by

$$\text{LR}(n) = \frac{\lambda}{\sqrt{d_h}} \min \left(\frac{n}{n_{\text{warmup}}^{1.5}}, \frac{1}{\sqrt{n}} \right), \quad (7)$$

where $\lambda = 400$, n_{warmup} are hyperparameters. However, such a decay led to early stagnation in validation accuracy, after which we divide the learning rate by 10 and run at the decayed rate for 20 epochs. We do this twice then take the model with the highest validation accuracy. Xavier initialization gave validation accuracies of zero for the first few epochs, suggesting room for improvement. Like previous works on self-attention, we apply label smoothing (see tables; we also tried model averaging, but to no gain). To compute word error rates (WER), we use the dataset’s provided language model (LM) as incorporated by WFST decoding [7] to bridge the gap between CTC and encoder-decoder frameworks, allowing comparison with known benchmarks and informing systems that incorporate expert knowledge in this manner (e.g., via a pronunciation lexicon).

Model	dev93		eval92	
	CER	WER	CER	WER
CTC (BRDNN) [5]	—	—	10.0	—
CTC (BLSTM) [4]	—	—	9.2	—
CTC (BLSTM) [17]	11.5	—	9.0	—
Enc-Dec (4-1) [17]	12.0	—	8.2	—
Enc-Dec+CTC (4-1) [17]	11.3	—	7.4	—
Enc-Dec (4-1) [37]	—	—	6.4	9.3
CTC/ASG (Gated CNN) [38]	6.9	9.5	4.9	6.6
Enc-Dec (2,1,3-1) [39]	—	—	3.6	—
CTC (SAN), reshape, additive	7.1	9.3	5.1	6.1
+ label smoothing, $\lambda = 0.1$	6.4	8.9	4.7	5.9

Table 2: End-to-end, MLE-based, open-vocab. models trained on WSJ. Only WERs incorporating the extended 3-gram LM or a 4-gram LM (Gated CNN) are listed.

Model	dev93		eval92	
	PER	WER	PER	WER
CTC (BRDNN) [7]	—	—	—	7.87
CTC (BLSTM) [11]	—	9.12	—	5.48
CTC (ResCNN) [11]	—	9.99	—	5.35
Ensemble of 3 (voting) [11]	—	7.65	—	4.29
CTC (SAN), reshape, additive	7.12	8.09	5.07	4.84
+ label smoothing, $\lambda = 0.1$	6.86	8.16	4.73	5.23

Table 3: CTC phoneme models with WFST decoding on WSJ.

3.1. Wall Street Journal (WSJ)

We train on the 80-hour WSJ corpus to validate our architectural choices. Similar to [17, 19], we use 40-dim. mel-scale filter banks and hence 120-dim. features. We warmup for 8000 steps, use a dropout of 0.2, and switch schedules at epoch 40. For the WSJ dataset, we compare with similar MLE-trained, end-to-end, open-vocabulary systems in Table 2, giving a best CER of 4.7%, outdoing previous results on CTC except [38] (4.6% with a trainable frontend). We use the provided extended 3-gram LM to compare WERs. We also compare against phoneme-based systems, which also incorporate the CMU pronunciation lexicon via WFST; results are in Table 3. These models trained in 1 day, comparable to the Speech Transformer [19]; however, SAN-CTC gives further benefits at inference time as token predictions are generated in parallel.

We also evaluate design choices in Table 4. Here, we consider the effects of downsampling and position encoding methods on accuracy for our fixed training regime. We see that unlike self-attentional LAS [27], SAN-CTC works respectably even with no position embeddings; in fact, the contribution of position is relatively minor (compare with [21], where location in an encoder-decoder improved CER by 3% absolute). Lossy downsampling preserves performance in CER, but degrades WER (as information about frame transitions is lost). These observations can be viewed as reflecting the monotonicity and independence assumptions of CTC.

Inspired by [27], we plot the standard deviation of attention weights for each head as training progresses; see Figure 2 for details. In our first layer, we observe a similar differentiation of variances, along with wide-context heads; in later layers, unlike [27] we see a smaller but still marked differentiation into groups in later layers. Inspired by [26], we further plot the attention weights relative to the current time position; here, per head. For characters, we see that forward and backward-attending heads are learned (averaging

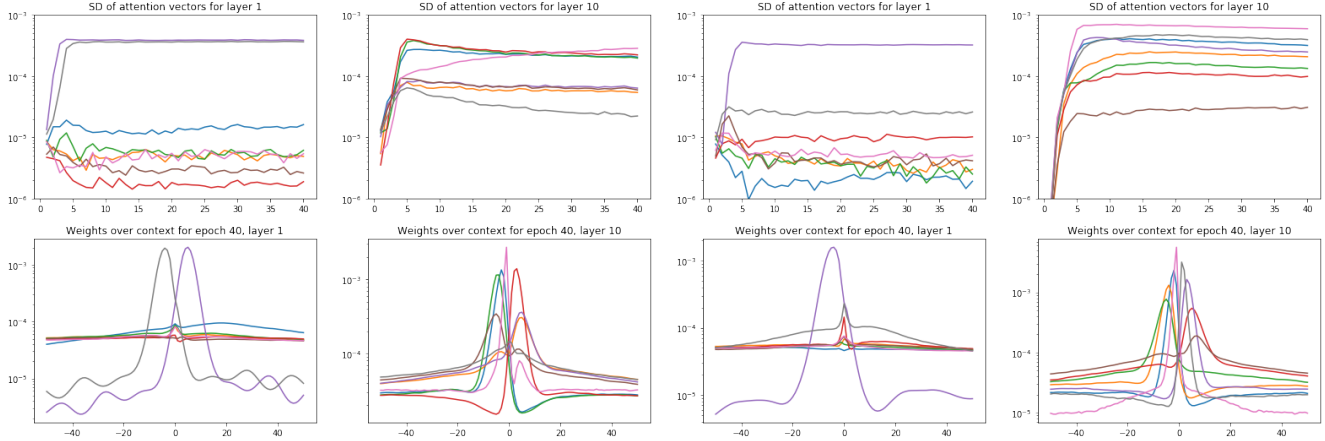


Fig. 2: Average attention weights over WSJ’s test set. The left half is a character model; the right half is a phoneme model. Each curve corresponds to a head, at layers 1 and 10, of representative SAN-CTC models (reshape + additive embedding). The first row charts standard deviation over time; the second row charts the attention magnitudes relative to position, where 0 represents attending to the same position.

Downsampling	Position embedding	dev93	
		CER	WER
reshape	content-only	7.62	9.57
reshape	additive	7.10	9.27
reshape	concatenative	7.10	9.97
pooling (maximum)	additive	7.15	10.72
pooling (average)	additive	6.82	9.41
subsample	additive	none	none

Table 4: SAN-CTC character model on WSJ with modifications

these would retrieve the bimodal distribution plotted in [26]), holding across layers. This suggests a gradual expansion of context over depth, as often engineered in purely-convolutional CTC; this also justifies using fewer heads, directed self-attention [25], and restricted contexts to accelerate training (Table 1). For comparison, phoneme training gives a single backward-attending head, along with more diffuse heads. We believe this is symptomatic of English characters as being far less conditionally independent than phonemes (e.g., emitting ‘tt’ requires looking ahead, to ensure a blank symbol prints between two runs of ‘t’ in the path).

3.2. LibriSpeech

We give the first large-scale demonstration of a self-attentional speech recognition model by using the LibriSpeech ASR corpus [40], an English corpus produced from audio books giving 960 hours of training data. We use 13-dim. mel-frequency cepstral coefficients and hence 39-dim. features. We double the warmup period, use a dropout of 0.1, and switch schedules at epoch 30. We attain a CER of 2.8%, which outdoes previous results except OCD training [39]. We use the provided 4-gram LM via WFST to compare WERs with current state-of-the-art, end-to-end, open-vocabulary systems in Table 5. Note that at this scale, label smoothing was detrimental given our schedule. Inspired by [34], we also trained the same architecture and schedule with BPE subwords as targets; however, we train from scratch. We took 300 merge operations, as 10k made training unstable, and attained a CER of 7.4%. Without an external language model, this gave a WER of 8.7% (compare with

Model	Tok.	test-clean		test-other	
		CER	WER	CER	WER
CTC/ASG (Wav2Letter) [9]	chr.	6.9	7.2	—	—
CTC (DS1-like) [31, 41]	chr.	—	6.5	—	—
Enc-Dec (4-4) [42]	chr.	6.5	—	18.1	—
Enc-Dec (6-1) [43]	chr.	4.5	—	11.6	—
CTC (DS2-like) [8, 30]	chr.	—	5.7	—	15.2
Enc-Dec+CTC (6-1, pretr.) [20]	10k	—	4.8	—	15.3
CTC/ASG (Gated CNN) [22]	chr.	—	4.8	—	14.5
Enc-Dec (2,6-1) [39]	10k	2.9	—	8.4	—
CTC (SAN), reshape, additive	chr.	3.2	5.2	9.9	13.9
+ label smoothing, $\lambda = 0.05$	chr.	3.5	5.4	11.3	14.5
CTC (SAN), reshape, concat.	chr.	2.8	4.8	9.2	13.1

Table 5: End-to-end, MLE-based, open-vocab. models trained on LibriSpeech. Only WERs incorporating the 4-gram LM are listed.

Table 5’s LM-based entries). For comparison, the best CTC-like architecture [22] takes 4-8 weeks on 4 GPUs¹ to attain its results. The Enc-Dec+CTC model takes 12.5 hours to iterate over all the data once on 1 GPU (GTX 1080 Ti)²; they train 12 iterations over the data over a runtime of 1 week. Our model takes 3 hours to iterate over all training data on 1 GPU (Tesla V100). We run 60 epochs in one week to get our results.

4. CONCLUSION

We introduced SAN-CTC, a novel architecture that successfully integrates self-attention layers with connectionist temporal classification loss. We address the challenges of reconciling the two approaches and adapting the architecture to speech recognition, and show SAN-CTC is competitive or outperforms existing end-to-end models on WSJ and LibriSpeech. Future work includes multitasking SAN-CTC with other decoders or streamlining network structure via directed attention or restricted context.

¹<https://github.com/facebookresearch/wav2letter/issues/11>

²<https://github.com/rwth-i6/returnn-experiments/tree/master/2018-asr-attention/librispeech/full-setup-attention>

5. REFERENCES

[1] A. Graves, S. Fernández, F. Gomez, and J. Schmidhuber, “Connectionist temporal classification: labelling unsegmented sequence data with recurrent neural networks,” in *Proc. Int. Conf. Mach. Learning (ICML)*. ACM, 2006, pp. 369–376.

[2] A. Graves and J. Schmidhuber, “Offline handwriting recognition with multidimensional recurrent neural networks,” in *Proc. Adv. Neural Inform. Process. Syst. (NIPS)*, 2009, pp. 545–552.

[3] D.-A. Huang, L. Fei-Fei, and J.C. Niebles, “Connectionist temporal modeling for weakly supervised action labeling,” in *Proc. Eur. Conf. Comput. Vision (ECCV)*, 2016, pp. 137–153.

[4] A. Graves and N. Jaitly, “Towards end-to-end speech recognition with recurrent neural networks,” in *Proc. Int. Conf. Mach. Learning (ICML)*. ACM, 2014, pp. 1764–1772.

[5] A.Y. Hannun, A.L. Maas, D. Jurafsky, and A.Y. Ng, “First-pass large vocabulary continuous speech recognition using bi-directional recurrent DNNs,” *CoRR*, vol. abs/1408.2873, 2014.

[6] A.L. Maas, Z. Xie, D. Jurafsky, and A.Y. Ng, “Lexicon-free conversational speech recognition with neural networks,” in *Proc. Conf. North Amer. Ch. Assoc. Comput. Linguistics Human Lang. Technol. (NAACL-HLT)*, 2015, pp. 345–354.

[7] Y. Miao, M. Gowayyed, and F. Metze, “EESEN: End-to-end speech recognition using deep RNN models and WFST-based decoding,” in *Proc. IEEE Autom. Speech Recognition Understanding Workshop (ASRU)*. IEEE, 2015, pp. 167–174.

[8] D. Amodei, S. Anthanarayanan, R. Anubhai, J. Bai, E. Battenberg, C. Case, J. Casper, B. Catanzaro, Q. Cheng, G. Chen, et al., “Deep Speech 2: End-to-end speech recognition in English and Mandarin,” in *Proc. Int. Conf. Mach. Learning (ICML)*. ACM, 2016, pp. 173–182.

[9] R. Collobert, C. Puhrsch, and G. Synnaeve, “Wav2Letter: an end-to-end ConvNet-based speech recognition system,” *CoRR*, vol. abs/1609.03193, 2016.

[10] Y. Zhang, M. Pezeshki, P. Brakel, S. Zhang, C. Laurent, Y. Bengio, and A. C. Courville, “Towards end-to-end speech recognition with deep convolutional neural networks,” in *Proc. Ann. Conf. Int. Speech Communication Assoc. (INTERSPEECH)*, 2016, pp. 410–414.

[11] Y. Wang, X. Deng, S. Pu, and Z. Huang, “Residual convolutional CTC networks for automatic speech recognition,” *CoRR*, vol. abs/1702.07793, 2017.

[12] A.J. Robinson, “An application of recurrent nets to phone probability estimation,” *IEEE Trans. Neural Netw.*, vol. 5, no. 2, pp. 298–305, 1994.

[13] I. Sutskever, O. Vinyals, and Q.V. Le, “Sequence to sequence learning with neural networks,” in *Proc. Adv. Neural Inform. Process. Syst. (NIPS)*, 2014, pp. 3104–3112.

[14] D. Bahdanau, K. Cho, and Y. Bengio, “Neural machine translation by jointly learning to align and translate,” *CoRR*, vol. abs/1409.0473, 2014.

[15] W. Chan, N. Jaitly, Q.V. Le, and O. Vinyals, “Listen, attend and spell: A neural network for large vocabulary conversational speech recognition,” in *Proc. IEEE Int. Conf. Acoustics Speech Signal Process. (ICASSP)*. IEEE, 2016, pp. 4960–4964.

[16] Y. Zhang, W. Chan, and N. Jaitly, “Very deep convolutional networks for end-to-end speech recognition,” in *Proc. IEEE Int. Conf. Acoustics Speech Signal Process. (ICASSP)*. IEEE, 2017, pp. 4845–4849.

[17] S. Kim, T. Hori, and S. Watanabe, “Joint CTC-attention based end-to-end speech recognition using multi-task learning,” in *Proc. IEEE Int. Conf. Acoustics Speech Signal Process. (ICASSP)*. IEEE, 2017, pp. 4835–4839.

[18] C.-C. Chiu, T.N. Sainath, Y. Wu, R. Prabhavalkar, P. Nguyen, Z. Chen, A. Kannan, R.J. Weiss, K. Rao, K. Gonina, et al., “State-of-the-art speech recognition with sequence-to-sequence models,” in *Proc. IEEE Int. Conf. Acoustics Speech Signal Process. (ICASSP)*. IEEE, 2018, pp. 4774–4778.

[19] L. Dong, S. Xu, and B. Xu, “Speech-transformer: a no-recurrence sequence-to-sequence model for speech recognition,” in *Proc. IEEE Int. Conf. Acoustics Speech Signal Process. (ICASSP)*. IEEE, 2018.

[20] A. Zeyer, K. Irie, R. Schlüter, and H. Ney, “Improved training of end-to-end attention models for speech recognition,” in *Proc. Ann. Conf. Int. Speech Communication Assoc. (INTERSPEECH)*, 2018.

[21] T. Hori, S. Watanabe, Y. Zhang, and W. Chan, “Advances in joint CTC-attention based end-to-end speech recognition with a deep CNN encoder and RNN-LM,” in *Proc. Ann. Conf. Int. Speech Communication Assoc. (INTERSPEECH)*, 2017.

[22] V. Liptchinsky, G. Synnaeve, and R. Collobert, “Letter-based speech recognition with gated ConvNets,” *CoRR*, vol. abs/1712.09444, 2017.

[23] J. Cheng, L. Dong, and M. Lapata, “Long short-term memory-networks for machine reading,” in *Proc. Conf. Empirical Methods Natural Lang. Process. (EMNLP)*, 2016, pp. 551–561.

[24] A. Vaswani, N. Shazeer, N. Parmar, J. Uszkoreit, L. Jones, A.N. Gomez, Ł. Kaiser, and I. Polosukhin, “Attention is all you need,” in *Proc. Adv. Neural Inform. Process. Syst. (NIPS)*, 2017, pp. 6000–6010.

[25] T. Shen, T. Zhou, G. Long, J. Jiang, S. Pan, and C. Zhang, “DiSAN: Directional self-attention network for RNN/CNN-free language understanding,” in *Proc. AAAI Conf. Artificial Intell. (AAAI)*, 2018.

[26] D. Povey, H. Hadian, P. Ghahremani, K. Li, and S. Khudanpur, “A time-restricted self-attention layer for ASR,” in *Proc. IEEE Int. Conf. Acoustics Speech Signal Process. (ICASSP)*. IEEE, 2018.

[27] M. Sperber, J. Niehues, G. Neubig, S. Stüber, and A. Waibel, “Self-attentional acoustic models,” in *Proc. Ann. Conf. Int. Speech Communication Assoc. (INTERSPEECH)*, 2018.

[28] S. Zhou, L. Dong, S. Xu, and B. Xu, “Syllable-based sequence-to-sequence speech recognition with the Transformer in Mandarin Chinese,” in *Proc. Ann. Conf. Int. Speech Communication Assoc. (INTERSPEECH)*, 2018.

[29] S. Zhou, S. Xu, and B. Xu, “Multilingual end-to-end speech recognition with a single Transformer on low-resource languages,” *CoRR*, vol. abs/1806.05059, 2018.

[30] Y. Zhou, C. Xiong, and R. Socher, “Improving end-to-end speech recognition with policy learning,” in *Proc. IEEE Int. Conf. Acoustics Speech Signal Process. (ICASSP)*, 2018, pp. 5819–5823.

[31] A.Y. Hannun, C. Case, J. Casper, B. Catanzaro, G. Diamos, E. Elsen, R. Prenger, S. Satheesh, S. Sengupta, A. Coates, et al., “Deep Speech: Scaling up end-to-end speech recognition,” *CoRR*, vol. abs/1412.5567, 2014.

[32] T.N. Sainath, O. Vinyals, A. Senior, and H. Sak, “Convolutional, long short-term memory, fully connected deep neural networks,” in *Proc. IEEE Int. Conf. Acoustics Speech Signal Process. (ICASSP)*. IEEE, 2015, pp. 4580–4584.

[33] Z. Xie, Z. Sun, L. Jin, Z. Feng, and S. Zhang, “Fully convolutional recurrent network for handwritten Chinese text recognition,” in *Proc. Int. Conf. Pattern Recognition (ICPR)*. IEEE, 2016, pp. 4011–4016.

[34] T. Zenkel, R. Sanabria, F. Metze, and A. Waibel, “Subword and crossword units for CTC acoustic models,” in *Proc. Ann. Conf. Int. Speech Communication Assoc. (INTERSPEECH)*, 2018, pp. 396–400.

[35] T. Chen, M. Li, Y. Li, M. Lin, N. Wang, M. Wang, T. Xiao, B. Xu, C. Zhang, and Z. Zhang, “MXNet: A flexible and efficient machine learning library for heterogeneous distributed systems,” *CoRR*, vol. abs/1512.01274, 2015.

[36] Daniel Povey, Arnab Ghoshal, Gilles Boulianne, Lukas Burget, Ondrej Glembek, Nagendra Goel, Mirko Hannemann, Petr Motlicek, Yanmin Qian, Petr Schwarz, et al., “The kaldi speech recognition toolkit,” in *IEEE 2011 workshop on automatic speech recognition and understanding*. IEEE Signal Processing Society, 2011, number EPFL-CONF-192584.

[37] D. Bahdanau, J. Chorowski, D. Serdyuk, P. Brakel, and Y. Bengio, “End-to-end attention-based large vocabulary speech recognition,” in *Proc. IEEE Int. Conf. Acoustics Speech Signal Process. (ICASSP)*, 2016, pp. 4945–4949.

[38] N. Zeghidour, N. Usunier, G. Synnaeve, R. Collobert, and E. Dupoux, “End-to-end speech recognition from the raw waveform,” in *Proc. Ann. Conf. Int. Speech Communication Assoc. (INTERSPEECH)*, 2018, pp. 781–785.

[39] S. Sabour, W. Chan, and M. Norouzi, “Optimal completion distillation for sequence learning,” *CoRR*, vol. abs/1810.01398, 2018.

[40] V. Panayotov, G. Chen, D. Povey, and S. Khudanpur, “LibriSpeech: an ASR corpus based on public domain audio books,” in *Proc. IEEE Int. Conf. Acoustics Speech Signal Process. (ICASSP)*. IEEE, 2015, pp. 5206–5210.

[41] Mozilla Foundation, “A journey to <10% word error rate,” <https://hacks.mozilla.org/2017/11/a-journey-to-10-word-error-rate/>, 2017.

[42] D. Liang, Z. Huang, and Z.C. Lipton, “Learning noise-invariant representations for robust speech recognition,” in *Proc. IEEE Spoken Language Technol. Workshop (SLT)*. IEEE, 2018.

[43] A. Sriram, H. Jun, S. Satheesh, and A. Coates, “Cold Fusion: Training seq2seq models together with language models,” in *Proc. Ann. Conf. Int. Speech Communication Assoc. (INTERSPEECH)*, 2018, pp. 387–391.